Computers and Concrete, *Vol.15, No.3 (2015) 337-355*
DOI: http://dx.doi.org/10.12989/cac.2015.15.3.337

Effect of shear deformation on adhesive stresses in plated concrete beams: Analytical solutions

Mahmoud Touati[1], Abdelouahed Tounsi[1, 2*] and Mohamed Benguediab[3]

[1]*Material and Hydrology Laboratory, University of Sidi Bel Abbes, Faculty of Technology, Civil Engineering Department, Algeria*
[2]*Laboratoire des Structures et Matériaux Avancés dans le Génie Civil et Travaux Publics, Université de Sidi Bel Abbes, Faculté de Technologie, Département de génie civil, Algeria*
[3]*Département de Mécanique, Faculté de Technologie, Université de Sidi Bel Abbes, Algeria*

(*Received December 7, 2014, Revised February 10, 2014, Accepted February 11, 2014*)

Abstract. In this scientific work, an improved analytical solution for adhesive stresses in a concrete beam bonded with the FRP plate is developed by including the effect of the adherend shear deformations. The analysis is based on the deformation compatibility approach where both the shear and normal stresses are assumed to be invariant across the adhesive layer thickness. The shear stress distribution is supposed to be parabolic across the depth of the adherends in computing the adhesive shear stress and Timoshenko′s beam theory is employed in predicting adhesive normal stress to consider the shear deformation. Numerical results from the present analysis are presented both to demonstrate the advantages of the present solution over existing ones and to illustrate the main characteristics of adhesive stress distributions.

Keywords: plated concrete beams; adhesive stress; shear deformation; FRP composites

1. Introduction

Structural beams made of reinforced concrete (RC) or metal can be strengthened by bonding steel or composite plates/sheets to tension surfaces and this technical method has been the topic of important research effort and has shown to be a highly effective retrofit method in civil and structural engineering (Teng *et al*. 2001; Cadei *et al*. 2004; Nehdi *et al*. 2008; Belakhdar *et al*. 2011; Lee *et al*. 2011; Panjehpour *et al*. 2014abc). It is largely accepted that in such a strengthened beam, one of the important failure modes is the plate end debonding of the bonded plate from concrete beam, which depends widely on the adhesive shear and normal stress concentration at the cut-off points of the plate (Teng *et al*. 2002). Many analytical and numerical works are developed the scientific literatures to predict the adhesive stresses, such as the elastic shear stress analysis approach by Mukhopadhyaya and Swamy (2001); the shear-lag approach by Triantafillou and Deskovic (1991), Ye (2001) and Leung *et al*. (2015); the staged analysis approach by Roberts (1989), Roberts and Haji-Kazemi (1989) and the deformation compatibility-based approach by Vilnay (1988), Taljsten (1997), Malek *et al*. (1998), Maalej and Bian (2001), Smith and Teng

*Corresponding author, Associate Professor, E-mail: tou_abdel@yahoo.com

http://www.techno-press.org/?journal=cac&subpage=8 ISSN: 1598-8198 (Print), 1598-818X (Online)

(2001), Teng *et al*. (2002), Tounsi and Benyoucef (2007), Cai *et al*. (2007), Benachour *et al*. (2008), Tounsi (2006), Tounsi *et al*. (2009), and Guenaneche *et al*. (2014).

In this work, an improved analytical model is proposed to predict the adhesive stress distributions in a plated beam by considering the adherends shear deformations effect. The effect of the shear deformation of the adherends on the adhesive shear stress is included by supposing a parabolic distribution of shear stress across the thickness of the beam and of the FRP plate. In determining the solution for adhesive normal stress, the shear deformation in adherends is accounted for in closed form by utilizing the Timoshenko's beam theory (Narayanamurthy *et al*., 2011; Berrabah *et al*. 2013). A verification of the present analytical method with other theoretical solutions is carried out through illustrative examples to prove the effect of shear deformation in adherends. The effect of material and geometric parameters of the adherends and adhesive on the present method is also presented through a parametric study.

2. Governing equations and simplified solutions

Consider a concrete beam of span L retrofitted by a thin plate of length L_p which may be made of steel or fibre-reinforced plastics, bonded together with an adhesive layer. The beam is simply supported and subjected to four points bending, as shown in Fig. 1. It is assumed that (1) all of the materials are linear elastic; (2) the normal and shear stresses in the adhesive layer are constant across it; (3) a parabolic shear stress through the depth of both the concrete beam and bonded plate is assumed.

The interfacial shear and normal stresses are denoted by $\tau(x)$ and $\sigma(x)$, respectively.

Interfacial stress studies accounting for the influence of adherend shear deformation (shear-lag effect) are scarce. However, it is reasonable to assume that the shear stresses, which develop in the adhesive, are continuous across the adhesive–RC beam/FRP panel interface. In addition, equilibrium requires the shear stress be zero at the free surface. The importance of including the shear-lag effect of the adherends was shown by several authors such as Adams and Wake (1986), Jones and Callinan (1979) and Tsai *et al*. (1998) in adhesive lap joints. Tounsi (2006) has extended this theory to study concrete beams strengthened by FRP plates. The basic assumption in this later study is a linear distribution of shear stress across the thickness of the RC beam and the

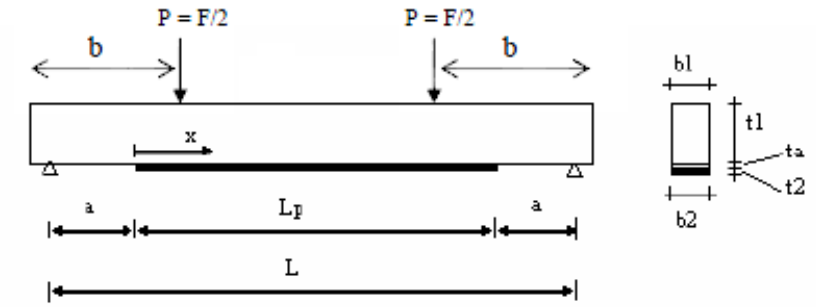

Fig. 1 Simply supported beam strengthened with bonded FRP plate

FRP plate. However, it is well known that, in beam theory, this distribution is parabolic through the depth of beam. Recently, Tounsi *et al*. (2009) have improved the method developed by Tounsi (2006) by assuming a parabolic shear stress across the depth of both FRP plate and RC beams. In the present study, the theory developed by Tounsi *et al*. (2009) is improved by considering the first order beam theory in predicting interfacial normal stress.

2.1 Shear stress distribution along the FRP–beam interface

The strains at the base of RC beam and the top of FRP panel, considering all three components of axial, bending and adherend shear deformations, are given as (Tounsi *et al*., 2009)

$$\varepsilon_1(x)=\frac{du_1(x)}{dx}=\frac{y_1}{E_1I_1}M_1(x)+\frac{N_1(x)}{E_1A_1}+\frac{t_1}{4G_1}\frac{d\tau(x)}{dx} \tag{1}$$

$$\varepsilon_2(x)=\frac{du_2(x)}{dx}=\frac{-y_2}{E_2I_2}M_2(x)+\frac{N_2(x)}{E_2A_2}-\frac{5t_2}{12G_2}\frac{d\tau(x)}{dx} \tag{2}$$

where $u_1(x)$ and $u_2(x)$ are the longitudinal displacements at the base of adherend 1 and the top of adherend 2. $N(x)$ and $M(x)$ are the axial forces, bending moment in each elements (RC beam and FRP panel) while y_1 and y_2 are the distance from the bottom of beam and top of plate to their respective centroid. t_1 and t_2 are the depth of the RC beam and the FRP panel, respectively. A the cross – sectional area, I the second moment of area, E the elastic modulus, G_1 and G_2 are the transverse shear moduli of the RC beam and FRP panel, respectively.

The shear stress in the adhesive can be expressed as follows:

$$\tau_a=\tau(x)=K_S\left[u_2(x)-u_1(x)\right] \tag{3}$$

where $K_S=\dfrac{G_a}{t_a}$ is shear stiffness of the adhesive, G_a and t_a are shear modulus and thickness of the adhesive, respectively. Differentiating the above expression we obtain

$$\frac{d\tau(x)}{dx}=K_S\left[\frac{du_2(x)}{dx}-\frac{du_1(x)}{dx}\right] \tag{4}$$

Consideration of horizontal equilibrium gives (see Fig. 2):

$$\frac{dN_1(x)}{dx}=-b_2\tau(x) \tag{5}$$

$$\frac{dN_2(x)}{dx}=b_2\tau(x) \tag{6}$$

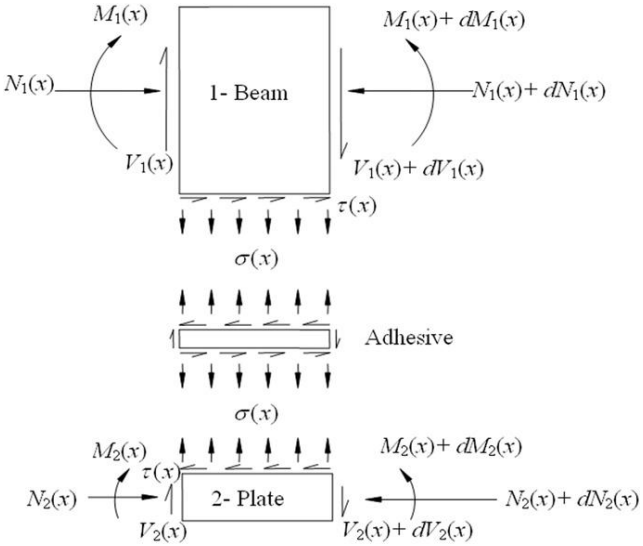

Fig. 2 Differential segment of a plated beam

where

$$N_2(x) = N(x) = b_2 \int_0^x \tau(x) \tag{7}$$

$$N_1(x) = -N(x) = -b_2 \int_0^x \tau(x) \tag{8}$$

b_2 is the width of the soffit plate.

Assuming equal curvature in the beam and soffit plate, the relationship between the moments in the two adherends can be expressed as

$$M_1(x) = RM_2(x) \tag{9}$$

with

$$R = \frac{E_1 I_1}{E_2 I_2} \tag{10}$$

Moment equilibrium of the differential segment of the plated beam in Fig. 2 gives

$$M_T(x) = M_1(x) + M_2(x) + N(x)[y_1 + y_2 + t_a] \tag{11}$$

where, $M_T(x)$ is the total applied moment.

The bending moment in each adherend, expressed as a function of the total applied moment and the interfacial shear stress, is given as

$$M_1(x)=\frac{R}{R+1}\left[M_T(x)-b_2\int_0^x\tau(x)(y_1+y_2+t_a)dx\right] \tag{12}$$

and

$$M_2(x)=\frac{1}{R+1}\left[M_T(x)-b_2\int_0^x\tau(x)(y_1+y_2+t_a)dx\right] \tag{13}$$

The first derivative of the bending moment in each adherend gives:

$$\frac{dM_1(x)}{dx}=\frac{R}{R+1}\left[V_T(x)-b_2\tau(x)(y_1+y_2+t_a)\right] \tag{14}$$

and

$$\frac{dM_2(x)}{dx}=\frac{1}{R+1}\left[V_T(x)-b_2\tau(x)(y_1+y_2+t_a)\right] \tag{15}$$

Substituting Eqs. (1) and (2) into Eq. (4) and differentiating the resulting equation once yields:

$$\begin{aligned}\frac{d^2\tau(x)}{dx^2}=&K_S\left(\frac{1}{E_2A_2}\frac{dN_2(x)}{dx}-\frac{y_2}{E_2I_2}\frac{dM_2(x)}{dx}-\frac{y_1}{E_1I_1}\frac{dM_1(x)}{dx}-\frac{1}{E_1A_1}\frac{dN_1(x)}{dx}\right)\\&-K_S\left(\frac{5t_2}{12G_2}+\frac{t_1}{4G_1}\right)\frac{d^2\tau(x)}{dx^2}\end{aligned} \tag{16}$$

Substitution of the shear forces (Eqs. (14) and (15)) and axial forces (Eq. (7) and (8)) into Eq. (16) gives the following governing differential equation for the interfacial stress

$$\frac{d^2\tau(x)}{dx^2}-K_1b_2\left(\frac{(y_1+y_2)(y_1+y_2+t_a)}{E_1I_1+E_2I_2}+\frac{1}{E_1A_1}+\frac{1}{E_2A_2}\right)\tau(x)+K_1\left(\frac{y_1+y_2}{E_1I_1+E_2I_2}\right)V_T(x)=0 \tag{17}$$

where

$$K_1=\frac{1}{\left(\dfrac{t_a}{G_a}+\dfrac{t_1}{4G_1}+\dfrac{5t_2}{12G_2}\right)} \tag{18}$$

For simplicity, the general solutions presented below are limited to loading which is either concentrated or uniformly distributed over part or the whole span of the beam, or both. For such loading, $d^2V_T(x)/dx^2 = 0$, and the general solution to Eq. (17) is given by:

$$\tau(x)=B_1\cosh(\lambda x)+B_2\sinh(\lambda x)+m_1V_T(x) \tag{19}$$

where

$$\lambda^2 = K_1 b_2 \left(\frac{(y_1 + y_2)(y_1 + y_2 + t_a)}{E_1 I_1 + E_2 I_2} + \frac{1}{E_1 A_1} + \frac{1}{E_2 A_2} \right) \tag{20}$$

and

$$m_1 = \frac{K_1}{\lambda^2} \left(\frac{y_1 + y_2}{E_1 I_1 + E_2 I_2} \right) \tag{21}$$

B_1 and B_2 are constant coefficients determined from the boundary conditions.

In the present study, a simply supported beam is investigated which is subjected to a two point loads symmetrically positioned. Two cases are considered: (1) the plate extends beyond the constant moment region (a<b) and (2) the plate is terminated within the constant moment region ($a > b$).

The general solution for the interfacial shear stress is given by the following expressions (Tounsi *et al*, 2009):

For a<b

$$\tau(x) = \begin{cases} \frac{m_2}{\lambda} Pae^{-\lambda x} - m_1 P \cosh(\lambda x) e^{-k} + m_1 P, & 0 \le x \le (b-a) \\ \frac{m_2}{\lambda} Pae^{-\lambda x} + m_1 P \sinh(k) e^{-\lambda x}, & (b-a) \le x \le \frac{L_p}{2} \end{cases} \tag{22}$$

For $a > b$

$$\tau(x) = \frac{m_2}{\lambda} Pbe^{-\lambda x}, \qquad 0 \le x \le L_P \tag{23}$$

where P is the concentrated load and $k = \lambda(b-a)$. The values of m_1 and m_2 take into consideration the shear deformation of the adherends.

2.2 Interfacial normal stress distribution along the FRP–beam interface

The interfacial normal stress in the adhesive can be expressed as follows:

$$\sigma_n(x) = K_n \Delta w(x) = K_n \left[w_2(x) - w_1(x) \right] \tag{24}$$

where K_n is normal stiffness of the adhesive per unit length and can be deduced as:

$$K_n = \frac{\sigma_n(x)}{\Delta w(x)} = \frac{\sigma_n(x)}{\Delta w(x)/t_a} \left(\frac{1}{t_a} \right) = \frac{E_a}{t_a} \tag{25}$$

$w_1(x)$ and $w_2(x)$ are the vertical displacements of adherend 1 and 2, respectively.

Differentiating Eq. (24) twice results in

$$\frac{d^2\sigma_n(x)}{dx^2} = K_n\left[\frac{d^2w_2(x)}{dx^2} - \frac{d^2w_1(x)}{dx^2}\right] \tag{26}$$

Considering the moment–curvature relationships for the beam to be strengthened and the external reinforcement, respectively:

$$\frac{d^2w_1(x)}{dx^2} = -\frac{1}{E_1I_1}M_1(x) - \frac{b_2}{G_1A_1\alpha_1}\sigma_n(x), \quad \frac{d^2w_2(x)}{dx^2} = -\frac{1}{E_2I_2}M_1(x) - \frac{b_2}{G_2A_2\alpha_2}\sigma_n(x) \tag{27}$$

where α_i (i=1, 2) is the Timoshenko's shear coefficient which is the ratio between the effective area resisting shear deformation and the actual cross sectional area of the adherend (e.g. $\alpha = 5/6$ for rectangle and $\alpha = 5/12$ for hollow thin walled square section).

The equilibrium of adherends 1 and 2, leads to the following relationships:

Adherend 1:

$$\frac{dV_1(x)}{dx} = -b_2\sigma_n(x) \qquad \frac{dM_1(x)}{dx} = V_1(x) - b_2y_1\tau(x) \tag{28}$$

Adherend 2:

$$\frac{dV_2(x)}{dx} = b_2\sigma_n(x) \qquad \frac{dM_2(x)}{dx} = V_2(x) - b_2y_2\tau(x) \tag{29}$$

Differentiating Eqs. (27) once with respect to x and substituting Eqs. (28) and (29) into the resulting equation gives

Adherend 1:

$$\frac{d^3w_1(x)}{dx^3} = -\frac{1}{E_1I_1}(V_1(x) - b_2y_1\tau(x)) - \frac{b_2}{G_1A_1\alpha_1}\frac{d\sigma_n(x)}{dx}; \tag{30}$$

Adherend 2:

$$\frac{d^3w_2(x)}{dx^3} = -\frac{1}{E_2I_2}(V_2(x) - b_2y_2\tau(x)) + \frac{b_2}{G_2A_2\alpha_2}\frac{d\sigma_n(x)}{dx}; \tag{31}$$

Differentiating Eqs. (30) and (31) once with respect to x and substituting Eqs. (28) and (29) into the resulting equation gives

Adherend 1:

$$\frac{d^4w_1(x)}{dx^4} = \frac{b_2}{E_1I_1}\sigma_n(x) - \frac{b_2}{G_1A_1\alpha_1}\frac{d^2\sigma_n(x)}{dx^2} + \frac{b_2y_1}{E_1I_1}\frac{d\tau(x)}{dx}; \tag{32}$$

Adherend 2:

$$\frac{d^4 w_2(x)}{dx^4} = -\frac{b_2}{E_2 I_2}\sigma_n(x) + \frac{b_2}{G_2 A_2 \alpha_2}\frac{d^2\sigma_n(x)}{dx^2} + \frac{b_2 y_2}{E_2 I_2}\frac{d\tau(x)}{dx}; \tag{33}$$

Differentiating Eq. (24) four times with respect to x and substituting Eqs. (33) and (32) into the resulting equation yields the following governing differential equation for the interfacial normal stress

$$\frac{d^4\sigma_n(x)}{dx^4} - \beta_1\frac{d^2\sigma(x)}{dx^2} + \beta_2\sigma(x) + \frac{E_a b_2}{t_a}\left(\frac{y_1}{E_1 I_1} - \frac{y_2}{E_2 I_2}\right)\frac{d\tau(x)}{dx} = 0 \tag{34}$$

where

$$\beta_1 = \frac{E_a b_2}{t_a}\left(\frac{1}{G_1 A_1 \alpha_1} + \frac{1}{G_2 A_2 \alpha_2}\right) \text{ and } \beta_2 = \frac{E_a b_2}{t_a}\left(\frac{1}{E_1 I_1} + \frac{1}{E_2 I_2}\right) \tag{35}$$

In Eq.(34), β_1 arose from Timoshenko's beam theory and represents the effect of shear deformation. If $\beta_1 = 0$ it reduces to the governing equation for interfacial normal stresses without considering shear deformation as in (Tounsi *et al*, 2009).

The governing equation for the interfacial normal stress given in Eq. (34) is a fourth order non-homogeneous ordinary differential equation. Its general solution can have the following three forms depending on the value of parameter d, which is influenced by material and geometric properties of the adherends and adhesive

$$\delta = 4\beta_2 - \beta_1^2 \tag{36}$$

For: $\delta > 0$

$$\sigma_n(x) = e^{-\eta_1 x}\left[C_1\cos(\eta_2 x) + C_2\sin(\eta_2 x)\right] + e^{+\eta_1 x}\left[C_{11}\cos(\eta_2 x) + C_{21}\sin(\eta_2 x)\right] - n_3\frac{d\tau(x)}{dx} \tag{37}$$

For: $\delta < 0$

$$\sigma_n(x) = C_3 e^{-\eta_3 x} + C_4 e^{-\eta_4 x} + C_{31} e^{\eta_3 x} + C_{41} e^{\eta_4 x} + n_8\frac{d\tau(x)}{dx} + n_9\frac{d^3\tau(x)}{dx^3} \tag{38}$$

For: $\delta = 0$

$$\sigma_n(x) = \left[C_5 + C_6 x\right]e^{-\eta_5 x} + \left[C_{51} + C_{61} x\right]e^{\eta_5 x} \tag{39}$$

where C_1 to C_6 and C_{11} to C_{61} are constants of integration. They are to be determined from appropriate boundary conditions and

$$\eta_1 = 0.5\sqrt{\beta_1 + 2\sqrt{\beta_2}}\ ; \eta_2 = \frac{\sqrt{\delta}}{4\eta_1};\ \ \eta_3 = \sqrt{0.5(\beta_1 + \sqrt{-\delta})} \tag{40a}$$

$$\eta_4 = \sqrt{0.5(\beta_1 - \sqrt{-\delta})};\ \ \eta_5 = \sqrt{0.5\beta_1};\ \ n_3 = \frac{n_2}{(\eta_1^2 + \eta_2^2)^2} \tag{40b}$$

$$n_4 = \frac{2\eta_1\eta_2}{(\eta_1^2 - \eta_2^2 - \beta_1)(3\eta_1^2\eta_2 - \eta_2^3 - \eta_2\beta_1) + (3\eta_1\eta_2^2 - \eta_1^3 - \eta_1\beta_1)(2\eta_1\eta_2)}; \tag{40c}$$

$$n_5 = \frac{1 - n_4(3\eta_1\eta_2^2 - \eta_2^3 - \eta_1\beta_1)}{\eta_1^2 + \eta_2^2 - \beta_1};\ \ n_6 = \frac{n_4(\eta_1^2 - \eta_2^2 - \beta_1)}{2\eta_1\eta_2} \tag{40d}$$

$$n_7 = \frac{3\eta_1\eta_2^2 - \eta_1^3 - \eta_1\beta_1}{\eta_1^2 - \eta_2^2 - \beta_1};\ \ n_8 = \frac{-n_2}{\eta_3^2\eta_4^2};\ \ n_9 = n_8\left(\frac{1}{\eta_3^2} + \frac{1}{\eta_4^2}\right) \tag{40e}$$

Because $\sigma(x) \to 0$ for large values of *x*, C_{11} to C_{61} = 0 and Eqs (40) reduce to

For: $\delta > 0$

$$\sigma_n(x) = e^{-\eta_1 x}\left[C_1\cos(\eta_2 x) + C_2\sin(\eta_2 x)\right] - n_3\frac{d\tau(x)}{dx} \tag{41}$$

For: $\delta < 0$

$$\sigma_n(x) = C_3 e^{-\eta_3 x} + C_4 e^{-\eta_4 x} + n_8\frac{d\tau(x)}{dx} + n_9\frac{d^3\tau(x)}{dx^3} \tag{42}$$

For: $\delta = 0$

$$\sigma_n(x) = \left[C_5 + C_6 x\right]e^{-\eta_5 x} \tag{43}$$

The constants C_1 to C_6 in Eqs. (41) to (43) are determined using the appropriate boundary conditions. The first boundary condition is the zero bending moment at the ends of the soffit plate, the second Boundary condition concerns the shear force at the end of the soffit plate in the beam and the soffit plate.

In the case of $\delta > 0$, differentiating Eq. (24) twice with respect to *x*, substituting Eq. (27) into the resulting expression gives:

$$\left.\frac{\partial^2\sigma(x)}{\partial x^2}\right|_{x=0} = \frac{E_a}{t_a}\left[-\frac{1}{E_2 I_2}M_2(0) + \frac{b_2}{G_2 A_2\alpha_2}\sigma_n(0) + \frac{1}{E_1 I_1}M_1(0) + \frac{b_2}{G_1 A_1\alpha_1}\sigma_n(0)\right] \tag{44}$$

Since it has been established that $M_2(0) = 0$ and $M_1(0) = M_T(0)$ at the end of the soffit plate, the above relationship can be expressed as:

$$\left.\frac{\partial^2\sigma(x)}{\partial x^2}\right|_{x=0} = \frac{E_a}{t_a E_1 I_1} M_T(0) + \beta_1 \sigma_n(0) \tag{45}$$

Setting x=0 in Eq. (41) and substituting in Eq. (44) gives:

$$\left.\frac{\partial^2\sigma(x)}{\partial x^2}\right|_{x=0} = \frac{E_a}{t_a E_1 I_1} M_T(0) + \beta_1 C_1 - \beta_1 n_3 \left.\frac{\partial\tau(x)}{\partial x}\right|_{x=0} \tag{46}$$

Differentiating Eq. (40) twice with respect to x and setting x=0 into the resulting equation gives:

$$\left.\frac{\partial^2\sigma(x)}{\partial x^2}\right|_{x=0} = (\eta_1^2 - \eta_2^2)C_1 - 2\eta_1\eta_2 C_2 - n_3 \left.\frac{\partial^3\tau(x)}{\partial x^3}\right|_{x=0} \tag{47}$$

From Eqs (46) and (47),

$$(\eta_1^2 - \eta_2^2 - \beta_1)C_1 - 2\eta_1\eta_2 C_2 = \frac{E_a}{t_a E_1 I_1} M_T(0) - n_3\left(\beta_1 \left.\frac{\partial\tau(x)}{\partial x}\right|_{x=0} - \left.\frac{\partial^3\tau(x)}{\partial x^3}\right|_{x=0}\right) \tag{48}$$

Differentiating Eq. (24) thrice with respect to x, substituting Eq. (30) and (31) into the resulting expression

$$\left.\frac{\partial^3\sigma(x)}{\partial x^3}\right|_{x=0} = \frac{E_a}{t_a}\left[-\frac{1}{E_2 I_2}(V_2(0) - b_2 y_2 \tau(0)) + \frac{b_2}{G_2 A_2 \alpha_2}\left.\frac{d\sigma_n(x)}{dx}\right|_{x=0} + \frac{1}{E_1 I_1}(V_1(0) - b_2 y_1 \tau(0)) + \frac{b_2}{G_1 A_1 \alpha_1}\left.\frac{d\sigma_n(x)}{dx}\right|_{x=0}\right] \tag{49}$$

Then applying the second boundary conditions, shear force at the end of the plate is zero $[V_2(0) = 0]$, $V_1(0) = V_T(0)$.

$$\left.\frac{\partial^3\sigma(x)}{\partial x^3}\right|_{x=0} = \left[\frac{E_a}{t_a E_1 I_1} V_T(0) + n_{2m}\tau(0) + \beta_1 \left.\frac{d\sigma_n(x)}{dx}\right|_{x=0}\right] \tag{50}$$

where

$$n_{2m} = \frac{E_a b_2}{t_a}\left(\frac{1}{E_2 I_2} y_2 - \frac{1}{E_1 I_1} y_1\right) \tag{51}$$

Differentiating Eq. (41) once with respect to x, setting x=0 and substituting the result into Eq. (50) gives

$$\left.\frac{\partial^3\sigma(x)}{\partial x^3}\right|_{x=0} = \left[\frac{E_a}{t_a E_1 I_1} V_T(0) + n_{2m}\tau(0) - \beta_1\eta_1 C_1 + \beta_1\eta_2 C_2 - \beta_1 n_3 \left.\frac{\partial^2\tau(x)}{\partial x^2}\right|_{x=0}\right] \tag{52}$$

Differentiating Eq. (41) three times with respect to x and setting x=0 gives

$$\left.\frac{\partial^3\sigma(x)}{\partial x^3}\right|_{x=0} = \left[2\eta_1\eta_2^2 - \eta_1\left(\eta_1^2 - \eta_2^2\right)\right]C_1 + \left[2\eta_1^2\eta_2 + \eta_2\left(\eta_1^2 - \eta_2^2\right)\right]C_2 - n_3\left.\frac{\partial^4\tau(x)}{\partial x^4}\right|_{x=0} \tag{53}$$

From Eqs. (52) and (53),

$$\left[3\eta_1\eta_2^2 - \eta_1^3 + \beta_1\eta_1\right]C_1 + \left[3\eta_1^2\eta_2 - \eta_2^3 - \beta_1\eta_2\right]C_2 = \left[\frac{E_a}{t_aE_1I_1}V_T(0) + n_{2m}\tau(0) - n_3\left(\beta_1\left.\frac{\partial^2\tau(x)}{\partial x^2}\right|_{x=0} - \left.\frac{\partial^4\tau(x)}{\partial x^4}\right|_{x=0}\right)\right] \tag{54}$$

C_1 and C_2 are obtained from Eqs (54) and (48) as

$$C_1 = \left(n_6 - n_4n_7\right)\left[\frac{E_a}{t_aE_1I_1}V_T(0) + n_{2m}\tau(0) - n_3\left(\beta_1\left.\frac{\partial^2\tau(x)}{\partial x^2}\right|_{x=0} - \left.\frac{\partial^4\tau(x)}{\partial x^4}\right|_{x=0}\right)\right] + n_5n_7\left[\frac{E_a}{t_aE_1I_1}M_T(0) - n_3\left(\beta_1\left.\frac{\partial\tau(x)}{\partial x}\right|_{x=0} - \left.\frac{\partial^3\tau(x)}{\partial x^3}\right|_{x=0}\right)\right] \tag{55}$$

$$C_2 = n_4\left[\frac{E_a}{t_aE_1I_1}V_T(0) + n_{2m}\tau(0) - n_3\left(\beta_1\left.\frac{\partial^2\tau(x)}{\partial x^2}\right|_{x=0} - \left.\frac{\partial^4\tau(x)}{\partial x^4}\right|_{x=0}\right)\right] - n_5\left[\frac{E_a}{t_aE_1I_1}M_T(0) - n_3\left(\beta_1\left.\frac{\partial\tau(x)}{\partial x}\right|_{x=0} - \left.\frac{\partial^3\tau(x)}{\partial x^3}\right|_{x=0}\right)\right] \tag{56}$$

3. Results and discussion

In this section, numerical results of the interfacial stresses in a beam bonded with the FRP plate are analyzed by considering the effect of the adherend shear deformations. In order to demonstrate the accuracy of the present analytical method, a comparison of the present results with those of Tounsi *et al* (2009) has been carried out. A steel plated RC beam of rectangular cross section under a four point bending with two transverse loads each of 30 kN as indicated in Fig. 3 is studied here as a typical case. The material and geometric properties of this beam are given in Table 1, which are taken from an experimental study reported by Jones *et al*. (1988).

The adhesive stresses from the above formulation are plotted in Fig. 4. It is observed that the present results are in excellent agreement with those of Tounsi *et al* (2006).

To better understand the behaviour of bonded beam repairs, which will help engineers in optimizing their design parameters, the effects of several parameters were studied. Fig. 5 prove that the peak adhesive stresses are significantly influenced by the magnitude of E_a: they are higher for stiffer adhesives.

Fig. 6 illustrates the variation of adhesive stresses for different thicknesses of the adhesive layer. Smaller adhesive stresses are found for thicker adhesive layer. However, design of the properties and thickness of the adhesive is a difficult problem. An optimization design of the adhesive is expected.

Fig. 7 proves that typical steel; CFRP and GFRP plates produce adhesive stresses in a decreasing order. The results demonstrate that, as the plate material becomes softer (from steel to CFRP and then GFRP), the adhesive stresses become smaller, as expected. This is because, under

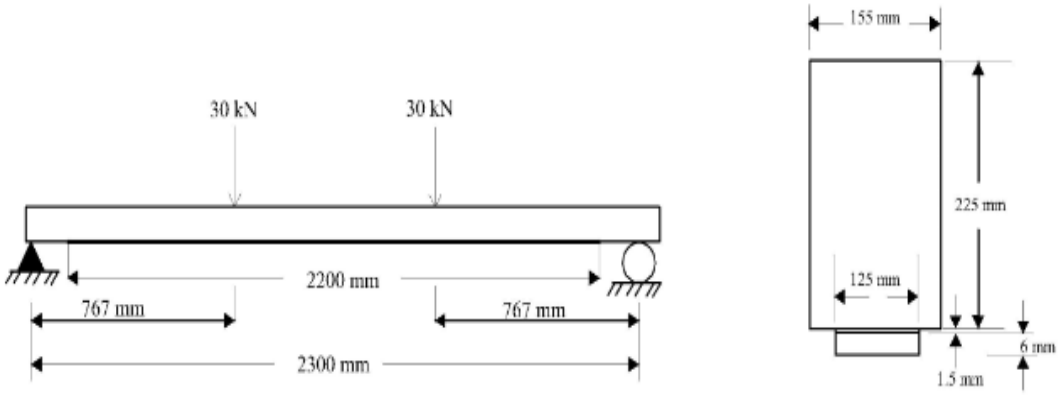

Fig. 3 A steel plated RC beam subjected to 4 point bending

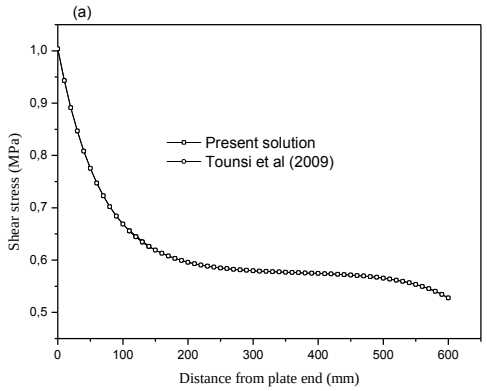

(a)

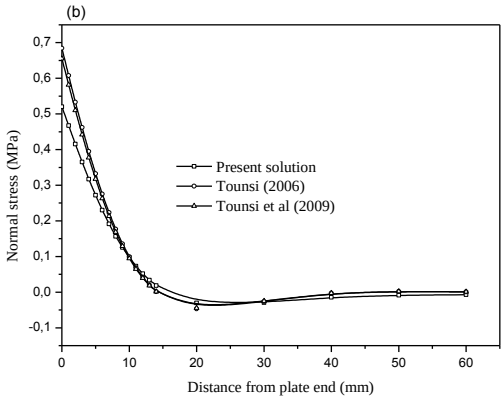

(b)

Fig. 4 Comparison of interfacial shear stress for steel-plated RC beam: (a) adhesive shear stress; (b) adhesive normal stress.

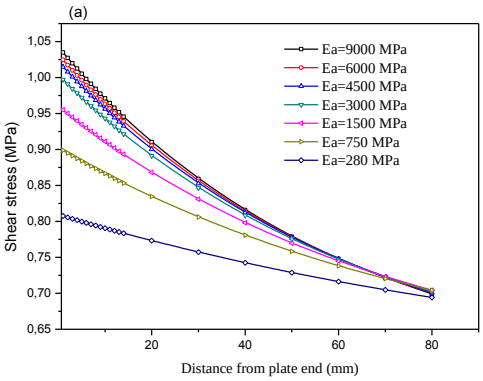

(a)

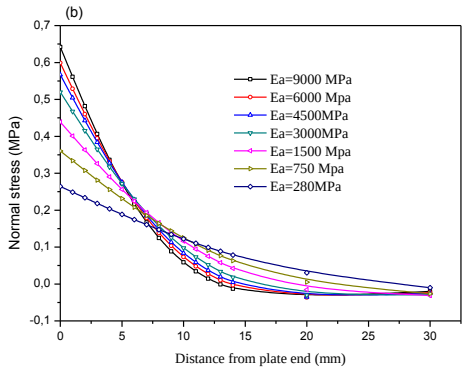

(b)

Fig. 5 Effect of adhesive thickness on interfacial stresses in a steel-plated RC beam under four point bending: (a) adhesive shear stress; (b) adhesive normal stress

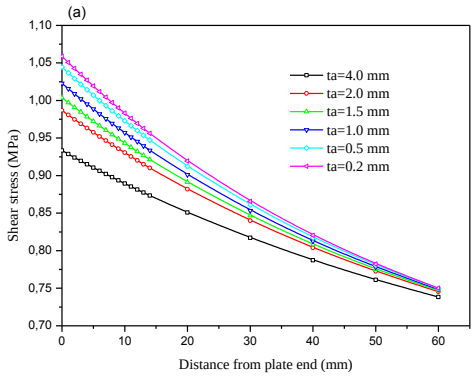

(a)

Fig. 6 Effect of adhesive thickness on interfacial stresses in a steel-plated RC beam under four point bending: (a) interfacial shear stress; (b) interfacial normal stress

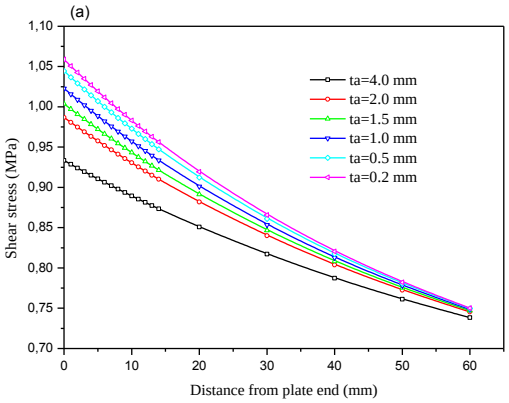

(b)

Fig. 6 Continued

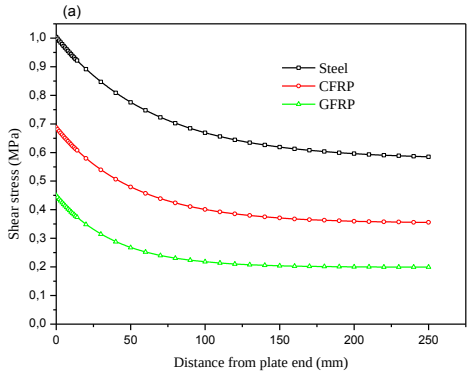

(a)

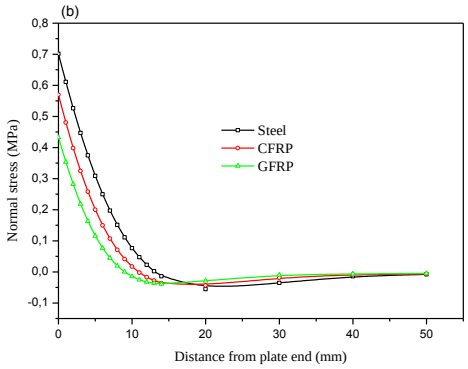

(b)

Fig. 7 Effect of plate material on interfacial stresses in a steel-plated RC beam under four point bending: (a) interfacial shear stress; (b) interfacial normal stress

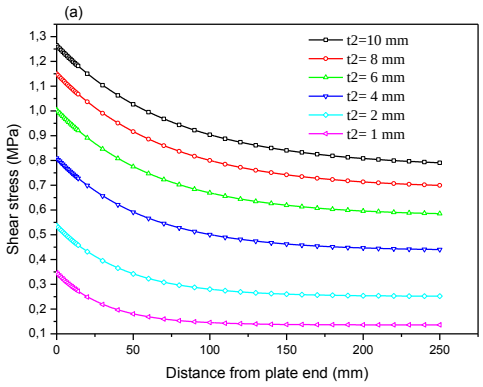

(a)

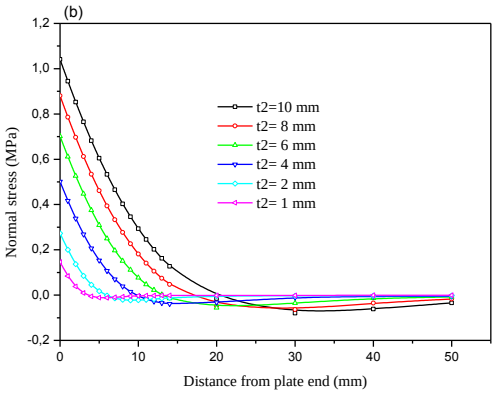

(b)

Fig. 8 Effect of plate thickness on interfacial stresses in a steel-plated RC beam under four point bending: (a) interfacial shear stress; (b) interfacial normal stress

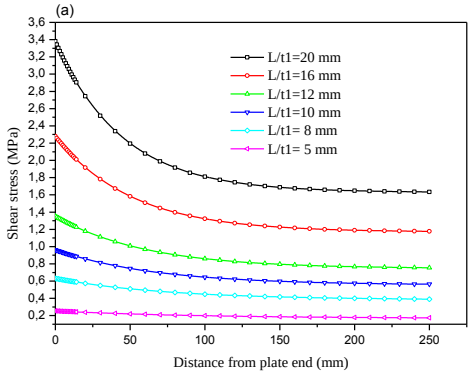

(a)

Fig. 9 Effect of span-to-depth ratio of beam on interfacial stresses in a steel-plated RC beam under four point bending: (a) interfacial shear stress; (b) interfacial normal stress

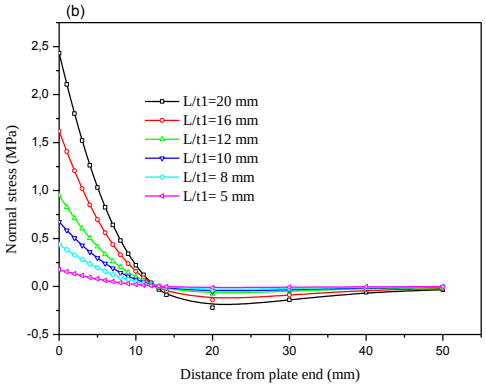

(b)

Fig. 9 Continued

Table 1 Geometric and material properties of example plated beams

Component	Width (mm)	Depth (mm)	Length (mm)	Elastic modulus (GPa)	Transverse shear modulus (GPa)
RC beam	$b_1 = 155$	$t_1 = 225$	$L_1 = 2300$	$E_1 = 31$	$G_1 = 31$
Steel plate	$b_2 = 125$	$t_2 = 125$	$L_2 = 2200$	$E_2 = 200$	$G_2 = 200$
Adhesive layer	$b_a = 125$	$t_a = 125$	$L_a = 2200$	$E_a = 3$	$G_a = 3$
CFRP plate	$b_2 = 125$	$t_2 = 125$	$L_2 = 2200$	$E_2 = 100$	$G_2 = 100$
GFRP plate	$b_2 = 125$	$t_2 = 125$	$L_2 = 2200$	$E_2 = 50$	$G_2 = 50$

the same load, the tensile force developed in the plate is smaller, which leads to reduced adhesive stresses. The position of the peak interfacial shear stress moves closer to the free edge as the plate becomes less stiff.

The influence of soffit plate thickness on the adhesive stresses is indicated in Fig. 8. A decrease in plate thickness decreases the adhesive stresses. Generally, the thickness of steel plates employed in practical engineering is high, compared with that of FRP plate. Therefore, the fact of the smaller interfacial stress level and concentration should be one of the advantages of retrofitting by FRP plate compared with a steel plate.

When the beam depth is reduced (the span-to-depth ratio L/t_1 is increased in Fig. 9), the adhesive stresses increases because the relative stiffness of the plate to beam increases.

4. Conclusions

In this work, an analytical plane stress solution for adhesive shear and normal stresses in plated beams is developed. The salient features of this method include the consideration of the effect of axial, bending and shear deformations in adherends. The influence of shear deformations in the adherends on adhesive shear stress is introduced by supposing that shear stress varies in a parabolic manner through the depth of the beam and the plate. Its effect on adhesive normal stress is included through Timoshenko's beam theory. The parametric study shows the influence of

different geometric and material properties of the plated beam on adhesive stresses. In future works, other beam theories such as higher order beam theories (Bouderba *et al*. 2013; Tounsi *et al*. 2013; Zidi *et al*. 2014; Belabed *et al*. 2014; Khalfi *et al*. 2014; Bousahla *et al*. 2014; Draiche *et al*., 2014; Hebali *et al*. 2014; Ait Amar Meziane *et al*. 2014; Bourada *et al*. 2015; Hamidi *et al*. 2015; Mahi *et al*. 2015) are expected to be included in adherends shear deformation effects to determine the adhesive normal stress.

References

Adams, R.D. and Wake, W.C. (1986), "Structural adhesive joints in engineering", Amsterdam: Elsevier, 1986.

Ait Amar Meziane, M., Abdelaziz, H.H. and Tounsi, A. (2014), "An efficient and simple refined theory for buckling and free vibration of exponentially graded sandwich plates under various boundary conditions", *J. Sandw. Struct. Mater.*, **16**(3), 293–318.

Belabed, Z., Houari, M.S.A., Tounsi, A., Mahmoud, S.R. and Anwar Bég, O. (2014), "An efficient and simple higher order shear and normal deformation theory for functionally graded material (FGM) plates", *Composites: Part B*, **60**, 274–283.

Belakhdar, K., Tounsi, A.,Adda Bedia E. and Redha, Y., (2011), "Effect of tapered-end shape of FRP sheets on stress concentration in strengthened beams", *Steel Compos. Struct.*, **11**(6), 435-454.

Benachour, A., Benyoucef, S., Tounsi, A. and Adda bedia, E.A. (2008), "Interfacial stress analysis of steel beams reinforced with bonded prestressed FRP plate", *Eng. Struct.*, **30**, 3305–3315.

Berrabah, H.M., Tounsi, A., Semmah, A. and Adda Bedia, E.A. (2013), "Comparison of various refined nonlocal beam theories for bending, vibration and buckling analysis of nanobeams", *Struct. Eng. Mech.*, **48**(3), 351 – 365.

Bouderba, B., Houari, M.S.A. and Tounsi, A. (2013) "Thermomechanical bending response of FGM thick plates resting on Winkler–Pasternak elastic foundations", *Steel Compos. Struct.*, **14**(1), 85 – 104.

Bourada, M., Kaci, A., Houari, M.S.A. and Tounsi, A. (2015), "A new simple shear and normal deformations theory for functionally graded beams", *Steel Compos. Struct.*, **18**(2), 409 – 423.

Bousahla, A.A., Houari, M.S.A., Tounsi, A. and Adda Bedia, E.A. (2014), "A novel higher order shear and normal deformation theory based on neutral surface position for bending analysis of advanced composite plates", *Int. J. Comput. Method*, **11**(6), 1350082.

Cadei, J.M.C., Stratford, T.J., Hollaway, L.C. and Duckett, W.G. (2004), "C595-Strengthening metallic structures using externally-bonded fibre-reinforced-polymers", London: CIRIA; 2004.

Cai, C.S., Nie, J. and Shi, X.M. (2007), "Interface slip effect on bonded plate repairs of concrete beams", *Eng. Struct.*, **29**,1084–1095.

Draiche, K., Tounsi, A. and Khalfi, Y. (2014), "A trigonometric four variable plate theory for free vibration of rectangular composite plates with patch mass", *Steel Compos. Struct.*, **17(1)**, 69-81.

Guenaneche, B., Tounsi, A. and Adda Bedia, E.A. (2014), "Effect of shear deformation on interfacial stress analysis in plated beams under arbitrary loading", *International Journal of Adhesion and Adhesives*, **48**, 1–13.

Hamidi, A., Houari, M.S.A., Mahmoud, S.R. and Tounsi, A. (2015), "A sinusoidal plate theory with 5-unknowns and stretching effect for thermomechanical bending of functionally graded sandwich plates", *Steel Compos. Struct.*, **18(1)**, 235 – 253.

Hebali, H., Tounsi, A., Houari, M.S.A., Bessaim, A. and Adda Bedia, E.A. (2014), "A new quasi-3D hyperbolic shear deformation theory for the static and free vibration analysis of functionally graded plates", *ASCE J. Eng. Mech.*, **140**, 374 – 383.

Jones, R. and Callinan, R.J. (1979), "Finite element analysis of patched cracks", *J. Struct. Mech.*, **7**, 107–130.

Jones, K.R, Swamy, R.N. and Charif, A. (1988), "Plate separation and anchorage of reinforced concrete beams strengthened by epoxy bonded steel plates", *Struct. Eng.*, **66**(5/1), 85–94.

Khalfi, Y., Houari, M.S.A. and Tounsi, A. (2014), "A refined and simple shear deformation theory for thermal buckling of solar functionally graded plates on elastic foundation", *Int. J. Comput. Method*, **11**(5), 135007.

Lee, H.K., Cheong, S.H., Ha, S.K. and Lee, C.G. (2011), "Behavior and performance of RC T-section deep beams externally strengthened in shear with CFRP sheets," *Compos. Struct.*, **93**(2), 911–922.

Leung, CKY. (2001), "Delamination failure in concrete beams retrofitted with a bonded plate", *J Mater Civil Eng ASCE*, **13**(2), 106–113.

Maalej, M. and Bian, Y. (2001), "Interfacial shear stress concentration in FRP strengthened beams", *Compos. Struct.*, **54**(4), 417-426.

Mahi, A., Adda Bedia, E.A., Tounsi, A. (2015), "A new hyperbolic shear deformation theory for bending and free vibration analysis of isotropic, functionally graded, sandwich and laminated composite plates", *Appl. Math. Modelling*, (In press)

Malek, A.M., Saadatmanesh, H. and Ehsani, M.R. (1998), "Prediction of failure load of R/C beams strengthened with FRP plate due to stress concentration at the plate end", *ACI Struct. J.*, **95**(1), 142–152.

Mukhopadhyaya, P. and Swamy, N. (2001), "Interfacial shear stress: a new design criteria for plate debonding", *J Compos. Constr.*, **5**, 35–43.

Narayanamurthy, V., Chen, J.F., Cairns, J. and Ramaswamy, A. (2011), "Effect of shear deformation on interfacial stresses in plated beams subjected to arbitrary loading", *Int. J. Adhes. Adhes.*, **31**, 862–874.

Nehdi, M., Omeman, Z. and El-Chabib, H. (2008), "Optimal efficiency factor in strut-and-tie model for FRP-reinforced concrete short beams with (1.5 < a/d < 2.5)," *Mater. Struct.*, **41**(10), 1713–1727.

Panjehpour, M., Ali, A.A.A., Voo, Y.L. and Aznieta, F.N. (2014a), "Effective compressive strength of strut in CFRP-strengthened reinforced concrete deep beams following ACI 318-11",*Comput. Concr.*, **13(1)**, 135-165.

Panjehpour, M., Ali, A.A.A. and Aznieta, F.N. (2014b), "Energy absorption of reinforced concrete deep beams strengthened with CFRP sheet", *Steel Compos. Struct.*, **16**(5), 481-489.

Panjehpour, M., Chai, H.K. and Voo, Y.L. (2014c), "Strut deformation in CFRP-strengthened reinforced concrete deep beams", *Scientific World J.*, 2014.

Roberts, T.M. (1989), "Approximate analysis of shear and normal stress concentrations in the adhesive layer of plated RC beams", *Struct. Eng.*, **67(12)**, 229–233.

Roberts, T.M. and Haji-Kazemi, H. (1989), "Theoretical study of the behavior of reinforced concrete beams strengthened by externally bonded steel plates", *Proceedings of the Institution of Civil Engineers*, **87**(2), 39–55.

Smith, S.T. and Teng, J.G. (2001), "Interfacial stresses in plated beams", *Engineering Structures*, **23**(7), 857–871.

Taljsten, B. (1997), "Strengthening of beams by plate bonding", *J Mater Civil Eng ASCE*, **9**(4), 206–212.

Teng, J.G., Chen, J.F., Smith, S.T. and Lam, L. (2001), "FRP strengthened RC structures", Chichester, UK: Wiley; 2001.

Teng, J.G., Chen, J.F., Smith, S.T. and Lam, L. (2002), "FRP-strengthened RC. Structures", West Sussex: Wiley; 2002.

Teng, J.G., Zhang, J.W. and Smith, S.T. (2002), "Interfacial stresses in reinforced concrete beams bonded with a soffit plate: a finite element study", *Constr. Build. Mater.*, **16(1)**, 1–14.

Tounsi, A. (2006), "Improved theoretical solution for interfacial stresses in concrete beams strengthened with FRP plate", *Int. J. Solids Struct.*, **43**, 4154–4174.

Tounsi, A. and Benyoucef, S. (2007), "Interfacial stresses in externally FRP plated concrete beams", *Int. J. Adhes. Adhes.*, **27**, 207–215.

Tounsi, A., Hassaine Daouadji, T., Benyoucef, S. and Adda Bedia, E.A. (2009), "Interfacial stresses in FRP—plated RC beams: effect of adherend shear deformations", *Int. J. Adhes. Adhes.*, **29**, 343–351.

Tounsi, A., Houari, M.S.A., Benyoucef, S. and Adda Bedia, E.A. (2013), "A refined trigonometric shear deformation theory for thermoelastic bending of functionally graded sandwich plates", *Aerosp. Sci. Tech.*, **24**, 209-220.

Triantafillou, T.C. and Deskovic, N. (1991), "Innovative prestressing with FRP sheets: mechanics of short-

term behavior", *J. Eng. Mech. ASCE*, **117**(7), 1652–1672.
Tsai, M.Y., Oplinger, D.W. and Morton, J. (1998), "Improved theoretical solutions for adhesive lap joints", *Int. J. Solids Struct.*, **35**(12), 1163–1185.
Vilnay, O. (1988), "The analysis of reinforced concrete beams strengthened by epoxy bonded steel plates", *Int. J. Cement Compos. Light- weight Concrete*, **10**(2), 73-78.
Ye, J.Q. (2001), "Interfacial shear transfer of RC beams strengthened by bonded composite plates", *Cement Concrete Compos*, **23**, 411-417.
Zidi, M., Tounsi, A., Houari, M.S.A., Adda Bedia, E.A. and Anwar Bég, O. (2014), "Bending analysis of FGM plates under hygro-thermo-mechanical loading using a four variable refined plate theory", *Aerosp. Sci. Tech.*, **34**, 24–34.

CC